Lensless Wiener–Khinchin telescope based on second-order spatial autocorrelation of thermal light

Zhentao Liu (刘震涛), Xia Shen (沈 夏), Honglin Liu (刘红林), Hong Yu (喻 虹), and Shensheng Han (韩申生)*

Key Laboratory for Quantum Optics, Shanghai Institute of Optics and Fine Mechanics, Chinese Academy of Sciences, Shanghai 201800, China

**Corresponding author: sshan@mail.shcnc.ac.cn*

Received January 21, 2019; accepted May 28, 2019; posted online August 2, 2019

The resolution of a conventional imaging system based on first-order field correlation can be directly obtained from the optical transfer function. However, it is challenging to determine the resolution of an imaging system through random media, including imaging through scattering media and imaging through randomly inhomogeneous media, since the point-to-point correspondence between the object and the image plane in these systems cannot be established by the first-order field correlation anymore. In this Letter, from the perspective of ghost imaging, we demonstrate for the first time, to the best of our knowledge, that the point-to-point correspondence in these imaging systems can be quantitatively recovered from the second-order correlation of light fields, and the imaging capability, such as resolution, of such imaging schemes can thus be derived by analyzing second-order autocorrelation of the optical transfer function. Based on this theoretical analysis, we propose a lensless Wiener–Khinchin telescope based on second-order spatial autocorrelation of thermal light, which can acquire the image of an object by a snapshot via using a spatial random phase modulator. As an incoherent imaging approach illuminated by thermal light, the lensless Wiener–Khinchin telescope can be applied in many fields such as X-ray astronomical observations.

OCIS codes: 110.1758, 110.6150, 350.1260, 290.5825.
doi: 10.3788/COL201917.091101.

Imaging resolution is an important metric of various imaging systems, including microscopy, astronomy, and photography[1–4]. It is well known that the operating wavelength λ and the aperture D of an imaging system are two key parameters for resolution[1,2]. Generally speaking, in conventional imaging systems, where a point-to-point correspondence between the object and the image plane can be established based on first-order field correlation, the resolution can be directly analyzed from a transmission function of the imaging system, and it is proportional to λ/D. Therefore, a shorter wavelength λ and/or a larger aperture D is required for a higher resolution; however, a large aperture leads to demanding requirements on the manufacture of a traditional monolithic optical telescope, which is arduous, especially for X-ray imaging.

Recently, emerging systems through random media[5–20] have been built, which include imaging through scattering media and imaging through randomly inhomogeneous media. However, it is challenging to determine the resolution of these imaging systems, since the point-to-point correspondence between the object and the image plane in these systems cannot be established by the first-order correlation anymore. In this Letter, we show that when the statistical properties of the random media are known as *a priori*, the resolution of such an imaging system can be deduced by analyzing the second-order correlation of light fields from the prospective of ghost imaging (GI)[10,21–23]. Based on this theoretical analysis, a lensless Wiener–Khinchin telescope is further proposed based on second-order spatial autocorrelation of thermal light, which can acquire the image of the object in a single shot by using a spatial random phase modulator. We demonstrate that different from conventional imaging systems, the resolution of imaging systems through random media not only depends on the aperture of random media, but also on the statistical properties of it in a theoretical and experimental way. The influence of signal bandwidth is also investigated. Moreover, experimental results for both far away and equivalent infinity far away imaging prove the feasibility of the proposed lensless Wiener–Khinchin telescope in astronomical observations.

The proposed lensless Wiener–Khinchin telescope (Fig. 1) consists of a spatial random phase modulator and a charge-coupled device (CCD) detector, which detects the intensity distribution of the modulated light field. The object is illuminated by a thermal light source.

For diffraction imaging[24], the spatial intensity distribution detected by the CCD detector is

$$I_t(r) = \int_{-\infty}^{\infty} \left\langle E_0(r_0,t)E_0^*(r_0',t)\right\rangle_t h_E(r;r_0)h_E^*(r;r_0')\mathrm{d}r_0\mathrm{d}r_0', \tag{1}$$

where $E_0(r_0,t)$ and $E_0(r_0',t)$ are the time-variant complex amplitude in the object plane, $h_E(r;r_0)$ and $h_E(r;r_0')$ are the point-spread function (PSF) of the imaging system, $\langle\cdot\rangle_t$ is the time average, r is the coordinate in the detection plane, and r_0 and r_0' are the coordinates in the object plane.

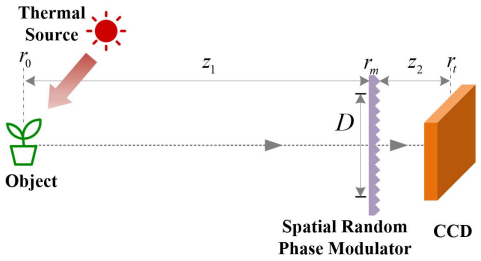

Fig. 1. Schematic of a lensless Wiener–Khinchin telescope. D is the diameter of the spatial random phase modulator. z_1 and z_2 are distances from the object and detection planes to the spatial random phase modulator, respectively.

Since the target of a telescope is illuminated by perfectly incoherent thermal light, we have[24]

$$\left\langle E_0(r_0,t)E_0^*(r_0',t)\right\rangle_t = \kappa I_0(r_0)\delta(r_0-r_0'), \tag{2}$$

where $I_0(r_0)=E_0(r_0)E_0^*(r_0)$ is the intensity distribution in the object plane, and κ is a real constant. Taking Eq. (2) into Eq. (1) yields

$$I_t(r)=\kappa\int_{-\infty}^{\infty} I_0(r_0)h_I(r;r_0)\mathrm{d}r_0, \tag{3}$$

where $h_I(r;r_0)=h_E(r;r_0)h_E^*(r;r_0)$ is the incoherent intensity impulse response function.

Considering the spatial random phase modulator for thermal light as an ergodic process, the second-order spatial autocorrelation of the measured light field is[25,26]

$$\begin{aligned} G_{I_t}^{(2)}(r+\Delta r,r) &= \langle E_t^*(r+\Delta r)E_t^*(r)E_t(r)E_t(r+\Delta r)\rangle_r \\ &= \overline{\{E_t^*(r+\Delta r)E_t^*(r)E_t(r)E_t(r+\Delta r)\}_s} \\ &= \overline{\left\{I_t(r)I_t(r+\Delta r)\right\}_s}, \end{aligned} \tag{4}$$

where $\langle\cdot\rangle_r$ is the spatial average over the coordinate r, and $\overline{\{\cdot\}}_s$ is the ensemble average of the spatial random phase modulator. Plugging Eq. (3) into Eq. (4), we have

$$\begin{aligned} G_{I_t}^{(2)}(r+\Delta r,r) = \iint_{-\infty} & G_h^{(2)}(r+\Delta r,r_0+\Delta r_0;r,r_0) \\ & \times I_0(r_0+\Delta r_0)I_0(r_0)\mathrm{d}r_0\mathrm{d}\Delta r_0, \end{aligned} \tag{5}$$

where

$$G_h^{(2)}(r+\Delta r,r_0+\Delta r_0;r,r_0)=\overline{\{h_E^*(r+\Delta r;r_0+\Delta r_0)h_E^*(r;r_0)h_E(r;r_0)h_E(r+\Delta r;r_0+\Delta r_0)\}_s} \tag{6}$$

is the second-order correlation function of PSFs between $h_E(r;r_0)$ and $h_E(r+\Delta r;r_0+\Delta r_0)$.

According to the central limit theorem[27], the light field $h_E(r;r_0)$ through the spatial random phase modulator obeys the complex circular Gaussian distribution in the spatial domain[27], and $G_h^{(2)}(r+\Delta r,r_0+\Delta r_0;r,r_0)$ can be written as[28]

$$\begin{aligned} & G_h^{(2)}(r+\Delta r,r_0+\Delta r_0;r,r_0) \\ & \quad = B[1+g_h^{(2)}(r+\Delta r,r_0+\Delta r_0;r,r_0)] \end{aligned} \tag{7}$$

with $B=\overline{\{h(r;r_0)\}_s}\,\overline{\{h(r+\Delta r;r_0+\Delta r_0)\}_s}$, and

$$\begin{aligned} & g_h^{(2)}(r+\Delta r,r_0+\Delta r_0;r,r_0) \\ & \quad = \frac{\left|\overline{\{h_E^*(r+\Delta r;r_0+\Delta r_0)h_E(r;r_0)\}_s}\right|^2}{B} \end{aligned} \tag{8}$$

is defined as the normalized second-order correlation of PSFs.

For Fresnel diffraction, the PSF of a lensless Wiener–Khinchin telescope is

$$\begin{aligned} h_E(r;r_0) = & \frac{\exp\left[j2\pi(z_1+z_2)/\lambda\right]}{-\lambda^2 z_1 z_2} \\ & \times \exp\left[\frac{j\pi(r-r_0)^2}{\lambda(z_1+z_2)}\right]\int_{-\infty}^{\infty} P(r_m)t(r_m) \\ & \times \exp\left[\frac{j\pi(z_1+z_2)}{\lambda z_1 z_2}\left(r_m-\frac{z_1 r+z_2 r_0}{z_1+z_2}\right)^2\right]\mathrm{d}r_m, \end{aligned} \tag{9}$$

where $P(r_m)$ and $t(r_m)=\exp[j2\pi(n-1)\eta(r_m)/\lambda]$ are the pupil function and the transmission function of the spatial random phase modulator, respectively, while $\eta(r_m)$ and n are the height and the refractive index of the spatial random phase modulator, respectively.

Substituting Eq. (9) into Eq. (8) yields

$$\begin{aligned} & g_h^{(2)}(r+\Delta r,r_0+\Delta r_0;r,r_0) \\ & \quad \times \frac{1}{B}\left|\iint_{-\infty} P(r_m)P^*(r_m')\overline{\{t(r_m)t^*(r_m')\}_s}\right. \\ & = \exp\left[j\frac{\pi(z_1+z_2)}{\lambda z_1 z_2}\left(r_m-\frac{z_1 r+z_2 r_0}{z_1+z_2}\right)^2\right] \\ & \quad \times \exp\left\{-j\frac{\pi(z_1+z_2)}{\lambda z_1 z_2}\right. \\ & \quad \left.\left.\times\left[r_m'-\frac{z_1(r+\Delta r)+z_2(r_0+\Delta r_0)}{z_1+z_2}\right]^2\right\}\mathrm{d}r_m\mathrm{d}r_m'\right|^2. \end{aligned} \tag{10}$$

In general, assuming the height ensemble average $R_\eta(r_m,r_m')$ of the spatial random phase modulator obeys the following mathematical form[29]:

$$R_\eta(r_m, r'_m) = \overline{\{\eta(r_m)\eta(r'_m)\}_s} = \omega^2 \exp\left[-\left(\frac{r_m - r'_m}{\zeta}\right)^2\right] = R_\eta(\Delta r_m),\ \Delta r_m = r_m - r'_m, \tag{11}$$

where ω and ζ are the height standard deviation and the transverse correlation length of the spatial random phase modulator, respectively. Thus, we obtain (see Supplementary Materials for details)

$$g_h^{(2)}(r+\Delta r, r_0+\Delta r_0; r, r_0) \approx \left|\left\{\exp\left\{-2\left[\frac{2\pi(n-1)}{\lambda}\right]^2\left[\omega^2 - R_\eta\left(\frac{2\lambda z_1 z_2}{z_1+z_2}\nu\right)\right]\right\} \otimes \mathscr{F}\left\{\left|P(\mu)\right|^2\right\}_{\mu\to\nu}\right\}_{\frac{z_1\Delta r + z_2\Delta r_0}{2\lambda z_1 z_2}}\right|^2 = g_h^{(2)}\left(\frac{z_1\Delta r + z_2\Delta r_0}{2\lambda z_1 z_2}\right), \tag{12}$$

where $\mathscr{F}\{\cdots\}_{\mu\to\nu}$ represents the Fourier transform of the function with the variable μ, and the transformed function variable is ν.

Taking Eqs. (7) and (12) into Eq. (5), we have

$$G_{I_t}^{(2)}(r+\Delta r, r) \approx B\left\{\left[1 + g_h^{(2)}\left(\frac{\Delta r_0}{2\lambda z_1}\right)\right] \otimes G_{I_0}^{(2)}(r_0+\Delta r_0, r_0)\right\}_{-\frac{z_1}{z_2}\Delta r}, \tag{13}$$

where

$$G_{I_0}^{(2)}(r_0+\Delta r_0, r_0) = \left\langle I_0(r_0+\Delta r_0) I_0(r_0)\right\rangle_{r_0} = \int_{-\infty}^{\infty} I_0(r_0) I_0(r_0+\Delta r_0)\mathrm{d}r_0 \tag{14}$$

and

$$g_h^{(2)}\left(\frac{\Delta r_0}{2\lambda z_1}\right) = \left|\left\{\exp\left\{-2\left[\frac{2\pi(n-1)}{\lambda}\right]^2\left[\omega^2 - R_\eta\left(\frac{2\lambda z_1 z_2}{z_1+z_2}\nu\right)\right]\right\} \otimes \mathscr{F}\left\{\left|P(\mu)\right|^2\right\}_{\mu\to\nu}\right\}_{\frac{\Delta r_0}{2\lambda z_1}}\right|^2. \tag{15}$$

According to the Wiener–Khinchin theorem for deterministic signals[30] (also known as the autocorrelation theorem[31]), we have

$$G_{I_0}^{(2)}(r_0+\Delta r_0, r_0) = \mathscr{F}^{-1}\{|\mathscr{F}\{I_0(r_0)\}_{r_0\to f_0}|^2\}_{f_0\to\Delta r_0}. \tag{16}$$

Substituting Eq. (16) into Eq. (13), we obtain

$$G_{I_t}^{(2)}(r+\Delta r, r) \propto \left\{\left[1 + g_h^{(2)}\left(\frac{\Delta r_0}{2\lambda z_1}\right)\right] \otimes \mathscr{F}^{-1}\left\{\left|\mathscr{F}\{I_0(r_0)\}_{r_0\to f_0}\right|^2\right\}_{f_0\to\Delta r_0}\right\}_{-\frac{z_1}{z_2}\Delta r}. \tag{17}$$

Equation (17) indicates that the energy spectral density $\left|\mathscr{F}\{I_0(r_0)\}_{r_0\to f_0}\right|^2$ of the intensity distribution $I_0(r_0)$ on the object plane can be separated from $G_{I_t}^{(2)}(r+\Delta r, r)$, and the resolution is determined by $g_h^{(2)}\left(\frac{\Delta r_0}{2\lambda z_1}\right)$. The image of $I_0(r_0)$ can be reconstructed by utilizing phase retrieval algorithms[32–36]. Here, only the amplitude information of the target is interested, which can be used as a constraint to significantly improve the speed and quality of reconstruction[37].

To quantify the imaging system, the relationship between the field of view (FOV), the resolution, and the spatial random phase modulator is analyzed.

The space translation invariance of the system in space (also known as the memory effect[38–40]) is required in the lensless Wiener–Khinchin telescope; therefore, its FOV is limited by the memory effect range of the imaging system. Since the target of a telescope is very small compared with the imaging distance, the memory effect in its FOV is satisfied. The corresponding normalized second-order correlation function of light fields between different incident angles without transverse translation is (see Supplementary Materials for details)

$$g_\theta^{(2)}(\Delta\theta) = \exp\left\{-\left[\frac{2\pi\omega}{\lambda}\left(\sqrt{n^2 - \sin^2(\Delta\theta_i)} - n\right)\right]^2\right\} \approx \exp\left\{-\left[\frac{\pi n\omega}{\lambda}\sin^2(\Delta\theta)\right]^2\right\}, \tag{18}$$

where $\Delta\theta$ is the variation of the incident angle. According to Eq. (18), the FOV of the lensless Wiener–Khinchin telescope is proportional to $\frac{\lambda}{\omega}$.

In addition, Eq. (17) leads to a limitation of the FOV of the lensless Wiener–Khinchin telescope,

$$\mathrm{FOV} < \frac{L}{z_2} \tag{19}$$

with L denoting the CCD detector size. This equation indicates that the FOV is also limited by the CCD detector size. In order to obtain a large FOV, the CCD detector size of the lensless Wiener–Khinchin telescope is required to be much larger than $\frac{\lambda z_2}{\omega}$ in Eq. (18).

Equation (15) indicates that the resolution not only depends on the aperture of the spatial random phase modulator, but also the statistical properties of it. According to the convolution operation in $g_h^{(2)}\left(\frac{\Delta r_0}{2\lambda z_1}\right)$, we discuss two simple cases below, where the resolution is mainly limited by

the aperture and the statistical properties of the spatial random phase modulator, respectively.

Case 1: Resolution is mainly limited by the aperture.

When the full width at half-maximum (FWHM) of $\exp\left\{-2\left[\frac{2\pi(n-1)}{\lambda}\right]^2\left[\omega^2 - R_\eta\left(\frac{2\lambda z_1 z_2}{z_1+z_2}\nu\right)\right]\right\}$ is much smaller than the FWHM of $\mathscr{F}\{|P(\mu)|^2\}_{\mu\to\nu}$, we have

$$g_h^{(2)}\left(\frac{\Delta r_0}{2\lambda z_1}\right) \propto \left|\mathscr{F}\left\{|P(\mu)|^2\right\}_{\mu\to-\frac{\Delta r_0}{2\lambda z_1}}\right|^2. \tag{20}$$

For a circle aperture of the spatial random phase modulator, $P(\mu) = \mathrm{circ}\left(\frac{\mu}{D}\right)$, and this leads to

$$g_h^{(2)}\left(\frac{\Delta r_0}{2\lambda z_1}\right) \propto \left[\frac{J_1\left(\frac{2\pi D\Delta r_0}{z_1\lambda}\right)}{\frac{2\pi D\Delta r_0}{z_1\lambda}}\right]^2. \tag{21}$$

In this case, the resolution of the lensless Wiener–Khinchin telescope is proportional to $0.61\lambda z_1/D$.

Case 2: Resolution is mainly limited by the statistical properties.

When the FWHM of $\exp\left\{-2\left[\frac{2\pi(n-1)}{\lambda}\right]^2 \times \left[\omega^2 - R_\eta\left(\frac{2\lambda z_1 z_2}{z_1+z_2}\nu\right)\right]\right\}$ is much larger than the FWHM of $\mathscr{F}\left\{|P(\mu)|^2\right\}_{\mu\to\nu}$,

$$g_h^{(2)}\left(\frac{\Delta r_0}{2\lambda z_1}\right) \approx \exp\left\{-4\left[\frac{2\pi(n-1)\omega z_2\Delta r_0}{\lambda(z_1+z_2)\zeta}\right]^2\right\} \tag{22}$$

with the first-order approximation. In this case, the resolution is proportional to $\left(1+\frac{z_1}{z_2}\right)\frac{\lambda\zeta}{4\pi(n-1)\omega}$.

According to the analysis of the above two cases, **Case 1** requires $0.61\frac{\lambda z_1}{D} \gg \left(1+\frac{z_1}{z_2}\right)\frac{\lambda\zeta}{4\pi(n-1)\omega}$, namely $D \ll \frac{2.44\pi z_1 z_2(n-1)\omega}{(z_1+z_2)\zeta}$, while **Case 2** requires $D \gg \frac{2.44\pi z_1 z_2(n-1)\omega}{(z_1+z_2)\zeta}$.

For digital images, the reconstruction is also affected by the pixel size of the CCD detector. Due to Eq. (16), the pixel size P_{CCD} of the CCD detector is required by

$$P_{\mathrm{CCD}} < \frac{z_2}{Mz_1} g_h^{(2)}\left(\frac{\Delta r_0}{2\lambda z_1}\right), \tag{23}$$

where M denotes a split number for discrimination of the resolution. For **Case 1**, according to Eq. (20), the FWHM of $g_h^{(2)}\left(\frac{\Delta r_0}{2\lambda z_1}\right)$ is proportional to $\lambda z_1/D$, and taking this result into Eq. (22), the pixel size of the CCD detector is required to be smaller than $\frac{\lambda z_2}{MD}$. Similarly, for **Case 2**, the pixel size of the CCD detector is required to be smaller than $\frac{\lambda\zeta}{M(n-1)\omega}$ with $z_1 \gg z_2$ in a telescope scheme.

The experimental setup is shown in Fig. 2. An object is illuminated by a xenon lamp. The reflected light is filtered by a narrow-band filter and modulated by a spatial random phase modulator with a height standard deviation $\omega = 1$ μm, a transverse correlation length $\zeta = 22$ μm, and the refractive index $n = 1.46$, and then it is relayed by a lens, which has a 10× magnification, 0.25 numerical aperture, 195 mm conjugated distance, and 161 mm focus length, onto a CCD detector (APGCCD) with a pixel size 13 μm × 13 μm, which records the magnified intensity distribution. Usually, the width of the correlation of the intensity distribution is larger than two times the pixel size of the CCD. The lens is only used to amplify the intensity distribution to match the pixel size of the CCD detector and is not necessary in some conditions.

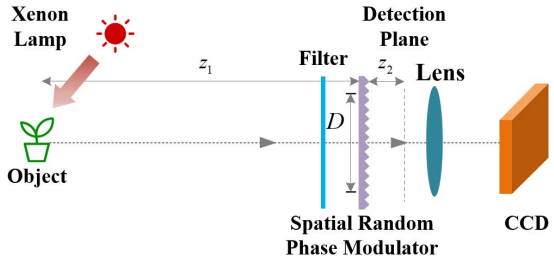

Fig. 2. Experimental setup of the lensless Wiener–Khinchin telescope.

In order to analyze the resolution of the system, a double slit [shown in Fig. 3(a)] is selected. Since the image is obtained from the second-order spatial autocorrelation of thermal light, the temporal coherence is not strictly required. But, the temporal coherence of the light field still affects the contrast of the spatial fluctuating pseudo-thermal light due to the dispersion of the spatial random phase modulator. The reflected light from the object is filtered by a narrow-band filter, whose central wavelength λ is either 532 or 550 nm, and its bandwidth w varies among 3, 10, 25, and 50 nm, when $z_1 = 0.15$ m, $z_2 = 12$ mm, and $D = 8$ mm. The results with the same

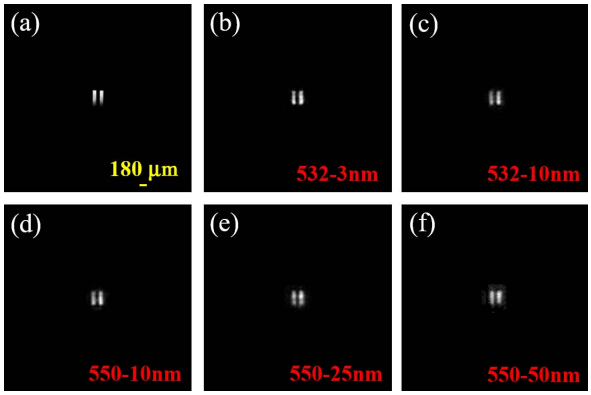

Fig. 3. Experimental results with different narrow-band filters. (a) A photograph of the double slit, where a yellow scale bar is inserted in the lower right corner. Reconstructed images with different narrow-band filters: (b) $\lambda = 532$ nm, $w = 3$ nm; (c) $\lambda = 532$ nm, $w = 10$ nm; (d) $\lambda = 550$ nm, $w = 10$ nm; (e) $\lambda = 550$ nm, $w = 25$ nm; (f) $\lambda = 550$ nm, $w = 50$ nm.

phase retrieval algorithm[34] are shown in Fig. 3. The experimental results show that the situation is better for narrow-band light. In subsequent experiments, a narrow-band filter with center wavelength $\lambda = 532$ nm and bandwidth $w = 10$ nm is selected.

To verify Eq. (21) in the experiment, the aperture size is changed. Images with five different values of apertures $D = 4$, 4.5, 5, 6, and 8 mm are obtained, respectively, while $z_1 = 1.1$ m and $z_2 = 60$ mm are selected approximately in accordance with **Case 1** [see Figs. 4(a)–4(e)]. According to Eq. (20), the theoretical resolutions with different apertures are shown in Fig. 4(f), where FWHMs for $D = 4$, 4.5, 5, 6, and 8 mm are 150, 134, 121, 100, and 75 μm, respectively. Figure 4(g) shows a comparison of theoretical and experimental resolutions at $D = 5$ mm, where the red dash line denotes a cross-section of the experimental result of the double slit in Fig. 4(c). The experimental results show that the double slit can be distinguished at $D = 5$ mm, which agrees well with the theoretical results.

In **Case 2**, the resolution is mainly affected by the statistical properties of the spatial random phase modulator, which leads to a limitation of z_2 based on Eq. (22). Five different values of z_2 (4, 6, 8, 10, and 12 mm) are selected, and the reconstructed images are shown in Figs. 5(a)–5(e), while $z_1 = 0.3$ m and $D = 8$ mm. The corresponding theoretical resolutions are shown in Fig. 5(f), where FWHMs for $z_2 = 4$, 6, 8, 10, and 12 mm are 156, 106, 80, 65, and 54 μm, respectively. Figure 5(g) shows a comparison of theoretical and experimental resolutions at $z_2 = 8$ mm, where the red dash line denotes a cross-section of the experimental result of the double slit in Fig. 5(c). The results show that the double slit can be distinguished at $z_2 = 8$ mm.

To further verify the imaging capability of the lensless Wiener–Khinchin telescope, two targets, a letter π and a panda toy, are imaged, respectively. The illumination is also a xenon lamp. Different system parameters are selected for the two targets at $D = 8$ mm. For the 'π', $z_1 = 0.5$ m, $z_2 = 2$ mm, and for the 'panda', $z_1 = 1.5$ m, $z_2 = 3$ mm. The reconstructed images of both are shown in Fig. 6.

For astronomical observations, the distance z_1 is nearly infinitely far away, which means $z_1 \gg z_2$, so the resolution $g_h^{(2)}\left(\frac{\Delta r_0}{2\lambda z_1}\right)$ in Eq. (15) is approximated to

$$g_h^{(2)}\left(\frac{\Delta r_0}{2\lambda z_1}\right) \propto \left|\left\{\exp\left\{-2\left[\frac{2\pi(n-1)}{\lambda}\right]^2[\omega^2 - R_\eta(2\lambda z_2 \nu)]\right\} \otimes \mathscr{F}\left\{\left|P(\mu)\right|^2\right\}_{\mu\to\nu}\right\}_{\frac{\Delta r_0}{2\lambda z_1}}\right|^2. \tag{24}$$

An object 'GI' is placed on the focal plane of an optical lens before the spatial random phase modulator to experimentally simulate the target placed infinitely far away. The image can be well reconstructed, as shown in Fig. 7. Imaging for both far and equivalently infinite far away demonstrated in Figs. 6 and 7 proves the feasibility of the lensless Wiener–Khinchin telescope in astronomical observations.

In conclusion, we present a novel theoretical framework for imaging schemes through random media and propose the lensless Wiener–Khinchin telescope based on second-order spatial autocorrelation of thermal light.

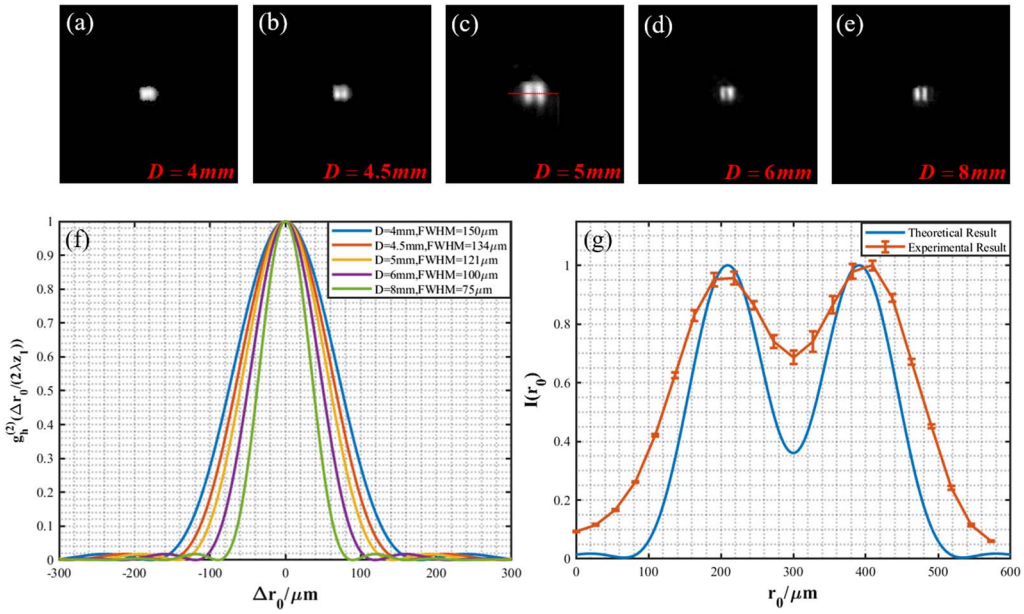

Fig. 4. Resolution at different apertures of the spatial random phase modulator. Reconstructed images with different apertures: (a) $D = 4$ mm, (b) $D = 4.5$ mm, (c) $D = 5$ mm, (d) $D = 6$ mm, (e) $D = 8$ mm. (f) The theoretical resolutions. (g) A comparison between theoretical and experimental resolutions at $D = 5$ mm, and the vertical red bar denotes a cross-section of the experimental result of the double slit in Fig. 4(c).

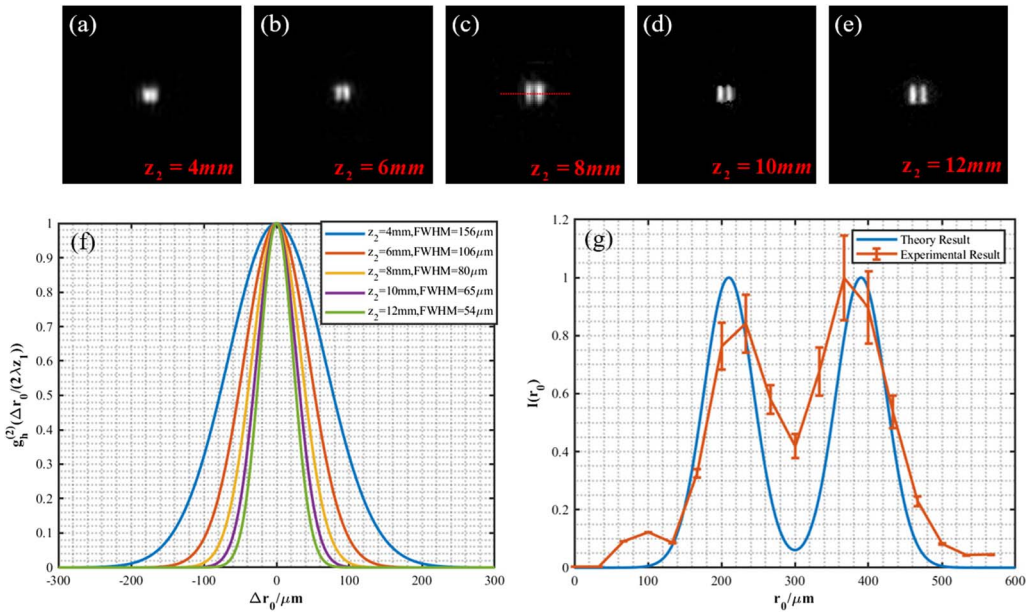

Fig. 5. Resolution at different z_2. Reconstructed images with different z_2: (a) $z_2 = 4$ mm, (b) $z_2 = 6$ mm, (c) $z_2 = 8$ mm, (d) $z_2 = 10$ mm, (e) $z_2 = 12$ mm. (f) The theoretical resolutions. (g) A comparison between the theoretical and experimental resolutions at $z_2 = 8$ mm, and the vertical red bar denotes a cross-section of the experimental result of the double slit in Fig. 5(c).

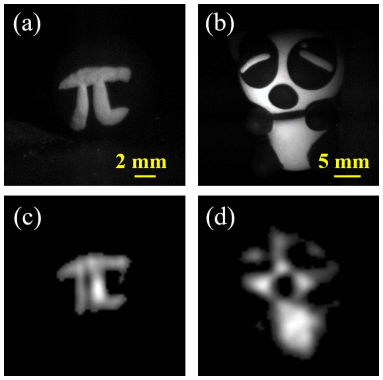

Fig. 6. Imaging of a letter π and a panda toy. (a) and (b) are photographs, where a yellow scale bar is inserted in the lower right corner, respectively. (c) and (d) are reconstructed images, respectively.

The attempt to extract spatial information of an object from high-order correlation of light fields can be traced back to the famous Hanbury Brown and Twiss (HBT) experiment in 1956[41,42], which is based on the second-order autocorrelation of light fields, and GI in 1995, which is based on second-order mutual correlation of light fields between the reference and test arms[43]. The HBT experiment and many of the early works of GI[44,45] perform ensemble statistics of the temporal fluctuating light field in the time domain, which requires that the temporal resolution of the detector is close to or less than the coherence time of the light field[46]. In contrast, by modulating true thermal light, such as sunlight, into a spatially fluctuating pseudo-thermal light field through a spatial random phase modulator[10], the lensless Wiener–Khinchin telescope based on second-order spatial autocorrelation of thermal light calculates the ensemble statistics of the spatially fluctuating pseudo-thermal light field in the spatial domain; therefore, the detection of the temporal intensity fluctuation is not required.

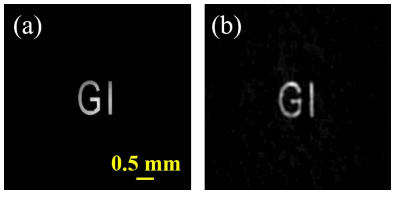

Fig. 7. Imaging an object placed equivalently infinite far away. (a) A photograph of the target, where a yellow scale bar is inserted in the lower right corner. (b) Reconstructed image.

On the other hand, from the viewpoint of the intensity autocorrelation, single-shot imaging through scattering layers and around corners via speckle correlations presented by Katz *et al.*[17] did not consider the diffraction effects of light through random phase modulation; therefore, the resolution of the imaging system can hardly be quantitatively calculated. By analyzing the second-order correlation of light fields, the resolution is derived and experimentally verified in the lensless Wiener–Khinchin telescope. The quantitative description of the imaging quality allows for such imaging systems to not only be demonstrated, but also be designed in practical applications.

Compared with lensless compressive sensing imaging[12,47,48] and lensless GI[46,49,50], neither a measurement matrix nor a calibration process is required. Thus, the lensless Wiener–Khinchin telescope has conspicuous advantages in applications such as X-ray astronomical observations,

where the measurement matrix or the calibration for an unknown imaging distance is difficult and less accurate. The cancellation of calibration also results in lower requirements in system stability. Moreover, considering the scattering media or the randomly inhomogeneous media as a spatial random phase modulator, the lensless Wiener–Khinchin telescope may also open a door to quantitatively describe imaging through scattering media or randomly inhomogeneous media[5,7–12,14–20].

We thank Guowei Li and Guohai Situ for helpful discussions. This work was supported by the National Key Research and Development Program of China (No. 2017YFB0503303) and the Hi-Tech Research and Development Program of China (Nos. 2013AA122902 and 2013AA122901).

References

1. C. J. R. Sheppard, Microsc. Res. Tech. **80**, 590 (2017).
2. S. Baker and T. Kanade, IEEE Trans. Pattern Anal. Mach. Intell. **24**, 1167 (2002).
3. M. C. Roggemann, B. M. Welsh, and R. Q. Fugate, Rev. Mod. Phys. **69**, 437 (1997).
4. X. Hao, C. Kuang, Z. Gu, Y. Wang, S. Li, Y. Ku, Y. Li, J. Ge, and X. Liu, Light: Sci. Appl. **2**, e108 (2013).
5. Y. Choi, T. D. Yang, C. Fang-Yen, P. Kang, K. J. Lee, R. R. Dasari, M. S. Feld, and W. Choi, Phys. Rev. Lett. **107**, 023902 (2011).
6. M. Bina, D. Magatti, M. Molteni, A. Gatti, L. A. Lugiato, and F. Ferri, Phys. Rev. Lett. **110**, 083901 (2013).
7. A. Liutkus, D. Martina, S. Popoff, G. Chardon, O. Katz, G. Lerosey, S. Gigan, L. Daudet, and I. Carron, Sci. Rep. **4**, 05552 (2014).
8. J. A. Newman and K. J. Webb, Phys. Rev. Lett. **113**, 263903 (2014).
9. H. Yilmaz, E. G. van Putten, J. Bertolotti, A. Lagendijk, W. L. Vos, and A. P. Mosk, Optica **2**, 424 (2015).
10. Z. Liu, S. Tan, J. Wu, E. Li, X. Shen, and S. Han, Sci. Rep. **6**, 25718 (2016).
11. S. K. Sahoo, D. Tang, and C. Dang, Optica **4**, 1209 (2017).
12. N. Antipa, G. Kuo, R. Heckel, B. Mildenhall, E. Bostan, R. Ng, and L. Waller, Optica **5**, 1 (2017).
13. B. Zhuang, C. Xu, Y. Geng, G. Zhao, H. Chen, Z. He, Z. Wu, and L. Ren, Chin. Opt. Lett. **16**, 041102 (2018).
14. P. Wang and R. Menon, Optica **2**, 933 (2015).
15. J. Bertolotti, E. G. van Putten, C. Blum, A. Lagendijk, W. L. Vos, and A. P. Mosk, Nature **491**, 232 (2012).
16. O. Katz, E. Small, and Y. Silberberg, Nat. Photon. **6**, 549 (2012).
17. O. Katz, P. Heidmann, M. Fink, and S. Gigan, Nat. Photon. **8**, 784 (2014).
18. X. Yang, Y. Pu, and D. Psaltis, Opt. Express **22**, 3405 (2014).
19. A. Labeyrie, Astron. Astrophys. **6**, 85 (1970).
20. D. Y. Gezari, A. Labeyrie, and R. V. Stachnik, Astrophys. J. **173**, L1 (1972).
21. H. Liu, J. Cheng, and S. Han, J. Appl. Phys. **102**, 103102 (2007).
22. P. Zhang, W. Gong, X. Shen, D. Huang, and S. Han, Opt. Lett. **34**, 1222 (2009).
23. Y. Shih, *Classical, Semi-classical and Quantum Noise* (Springer, 2011), p. 169.
24. J. W. Goodman, *Introduction to Fourier Optics* (Roberts, 2005), p. 132.
25. J. Cheng and S. Han, Phys. Rev. Lett. **92**, 093903 (2004).
26. J. H. Shapiro and R. W. Boyd, Quantum Inf. Process. **11**, 949 (2012).
27. J. W. Goodman, *Speckle Phenomena in Optics: Theory and Applications* (Roberts, 2007), p. 9.
28. J. W. Goodman, *Statistical Optics* (Wiley, 2015), p. 44.
29. S. K. Sinha, E. B. Sirota, S. Garoff, and H. B. Stanley, Phys. Rev. B **38**, 2297 (1988).
30. L. Cohen, in *Proceedings of the 1998 IEEE International Conference on Acoustics, Speech and Signal Processing* (IEEE, 1998).
31. J. W. Goodman, *Introduction to Fourier Optics* (Roberts, 2005), p. 8.
32. J. R. Fienup, Opt. Lett. **3**, 27 (1978).
33. J. R. Fienup, Appl. Opt. **21**, 2758 (1982).
34. X. Liu, J. Wu, W. He, M. Liao, C. Zhang, and X. Peng, Opt. Express **23**, 18955 (2015).
35. Y. Shechtman, Y. C. Eldar, O. Cohen, H. N. Chapman, J. Miao, and M. Segev, IEEE Sig. Process. Mag. **32**, 87 (2015).
36. J. Sun, Q. Qu, and J. Wright, Foundat. Computat. Mathe. **18**, 1131 (2017).
37. G. Ying, Q. Wei, X. Shen, and S. Han, Opt. Commun. **281**, 5130 (2008).
38. J. W. Goodman, *Introduction to Fourier Optics* (Roberts, 2005), p. 66.
39. S. Feng, C. Kane, P. A. Lee, and A. D. Stone, Phys. Rev. Lett. **61**, 834 (1988).
40. G. Osnabrugge, R. Horstmeyer, I. N. Papadopoulos, B. Judkewitz, and I. M. Vellekoop, Optica **4**, 886 (2017).
41. R. H. Brown and R. Q. Twiss, Nature **177**, 27 (1956).
42. T. A. Smith and Y. Shih, Phys. Rev. Lett. **120**, 063606 (2018).
43. D. V. Strekalov, A. V. Sergienko, D. N. Klyshko, and Y. H. Shih, Phys. Rev. Lett. **74**, 3600 (1995).
44. A. Valencia, G. Scarcelli, M. D'Angelo, and Y. Shih, Phys. Rev. Lett. **94**, 063601 (2005).
45. D. Zhang, Y. H. Zhai, L. A. Wu, and X. H. Chen, Opt. Lett. **30**, 2354 (2005).
46. X. F. Liu, X. H. Chen, X. R. Yao, W. K. Yu, G. J. Zhai, and L. A. Wu, Opt. Lett. **39**, 2314 (2014).
47. G. Huang, H. Jiang, K. Matthews, and P. Wilford, in *2013 IEEE International Conference on Image Processing* (IEEE, 2013).
48. M. S. Asif, A. Ayremlou, A. Sankaranarayanan, A. Veeraraghavan, and R. G. Baraniuk, IEEE Trans. Computat. Imag. **3**, 384 (2017).
49. X. H. Chen, Q. Liu, K. H. Luo, and L. A. Wu, Opt. Lett. **34**, 695 (2009).
50. H. Yu, R. Lu, S. Han, H. Xie, G. Du, T. Xiao, and D. Zhu, Phys. Rev. Lett. **117**, 113901 (2016).